TRGB Distances to the Andromeda Dwarf Satellites from the Isaac Newton Telescope Monitoring Survey

Hedieh Abdollahi*[1, 2]

[1]Konkoly Observatory, HUN-REN Research Centre for Astronomy and Earth Sciences, MTA Centre of Excellence, Konkoly-Thege Miklós út 15-17, H-1121, Budapest, Hungary
[2]School of Astronomy, Institute for Research in Fundamental Sciences (IPM), P.O. Box 1956836613, Tehran, Iran

Abstract

We measure tip of the red giant branch (TRGB) distances to 17 dwarf satellites of M31 from Sloan *i*-band photometry of the Isaac Newton Telescope (INT) monitoring survey of Local Group dwarf galaxies, and add the distances of And I, And VII and And IX from earlier papers of the survey. We locate the tip with a Sobel edge-detection filter applied to the luminosity function of stars within two half-light radii of each galaxy. The distance moduli range from 23.38 ± 0.06 mag (And XVI, 474 kpc) to 25.35 ± 0.06 mag (And XVIII, 1177 kpc), and 15 of the 20 satellites lie between 650 and 850 kpc. For most galaxies, our distance agrees with at least one published value. Compared with Conn et al. (2012), our tip is brighter for 12 of the 18 galaxies in common, by up to 0.39 mag, possibly because of crowding in the central regions. And XII lies at 844^{+40}_{-38} kpc, about 60 kpc behind M31, consistent with a first infall into the Local Group. And XXII lies at 753^{+28}_{-27} kpc, closer than all earlier estimates, and about 59 kpc from M33 in three dimensions (for an M33 distance of 794 kpc), consistent with an association with M33. And XVIII lies about 400 kpc behind M31, too far for a secure association with M31.

Keywords: *stars: luminosity function, mass function – galaxies: distances and redshifts – galaxies: dwarf – galaxies: stellar content – Local Group*

1. Introduction

The three-dimensional positions of the M31 satellites show how the satellite system is arranged and which galaxies belong to M31 or to M33. Their positions on the sky are known precisely, so the main uncertainty is their distance along the line of sight. For several of the fainter satellites, published distance moduli differ by a few tenths of a magnitude (Conn et al., 2012, McConnachie, 2012). At the distance of M31 (~ 780 kpc), a difference of 0.3 mag moves a satellite by about 110 kpc along the line of sight, enough to change whether it appears to lie near M31, near M33, or far from both. Distance alone cannot establish membership, but it is the first constraint, to be combined with kinematics. Reliable distances are also needed to compare the stellar populations of M31 and Milky Way satellites on the same basis.

The tip of the red giant branch (TRGB) is a standard distance indicator for resolved galaxies. It shows up as a sharp break in the luminosity function of the red giant branch, and in red optical bands its absolute magnitude varies little with age and metallicity in old, metal-poor populations (Lee et al., 1993). Conn et al. (2012) measured TRGB distances to most M31 satellites with a Bayesian method built for sparsely populated systems, and Savino et al. (2022) have since provided homogeneous RR Lyrae distances for most of them. Faint dwarfs remain difficult: few stars lie near the tip, and the result depends on the photometric depth, the extinction correction and the method used to find the edge. Published distances therefore differ partly because the data and analyses differ (Mahani et al., 2023). Measuring all satellites from one data set with one method reduces this source of scatter.

Our data come from the Isaac Newton Telescope (INT) monitoring survey of Local Group dwarf galaxies, which was designed to find long-period variable stars (LPVs) and study the evolved stellar populations of these systems (Saremi et al., 2020). LPVs trace their parent populations, because their luminosities, pulsation properties and evolutionary timescales are linked to the properties of their progenitor stars (Mahani

*hedieh.abdollahi@csfk.org

doi: https://doi.org/10.52526/25792776-26.73.2-322

et al., 2026). In M33, near-infrared LPV monitoring has been used to reconstruct the star-formation history of the centre and the disc (Javadi et al., 2011a,b, 2017) and to study dust production by evolved stars (Javadi et al., 2013). Similar work has been done for NGC 147 and NGC 185 (Mahani et al., 2025) and for NGC 6822 (Rostami & Mahani, 2025), using SED-fitting tools such as SEDust (Mahani & Javadi, 2026). The same INT images also give deep, uniform i-band photometry of the red giant branch, which we use here to measure TRGB distances.

The variable-star catalogue of the survey is published in Abdollahi et al. (2026a,b). Here, we present the TRGB distances of the observed M31 satellites, compare them with earlier estimates, and discuss three galaxies, And XII, And XXII and And XVIII, whose distances affect which systems belong to M31 or M33.

2. Observations and data

The observations were obtained with the Wide Field Camera (WFC) on the 2.5 m Isaac Newton Telescope at the Observatorio del Roque de los Muchachos, La Palma, between June 2015 and February 2018. The WFC consists of four 2048×4096 CCDs, with a pixel scale of 0.33 arcsec pixel^{-1}. Each galaxy was observed at multiple epochs in the Sloan i and Harris V filters. The survey strategy and the number of epochs for each galaxy are described in Saremi et al. (2020). Of the 24 M31 satellites in the survey sample, four (M110, M32, Pisces I and the Pegasus dwarf irregular, DDO 216) were not observed often enough for the variability analysis. And I, And VII and And IX were analysed in earlier papers of the survey (Abdollahi et al., 2023, Navabi et al., 2021, Saremi et al., 2021). We include their distances for completeness, so the final sample has 20 galaxies.

The images were reduced and aligned using the THELI pipeline (Erben et al., 2005). We performed the photometry with DAOPHOT/ALLSTAR and ALLFRAME (Stetson, 1987, 1994), which are well suited to the crowded fields of these galaxies, and calibrated the photometry using standard stars from Landolt (1992). For most galaxies, we used only CCD4, which covers approximately two half-light radii. For the more extended systems, such as And II (Abdollahi et al., 2024) and And XIX, we also used the other CCDs. Artificial-star tests show that the photometry is 90–95 per cent complete down to $i \approx 22$ mag, which is fainter than the TRGB in all targets except And XVIII, and about 50 per cent complete at $i \approx 23$ mag.

3. Measuring the TRGB

The TRGB marks the onset of core helium burning in low-mass red giants. In the Cousins I band, its absolute magnitude changes little with age and metallicity in old, metal-poor populations (Lee et al., 1993), and the tip has also been calibrated in the SDSS i band (Bellazzini, 2008). In the luminosity function, the tip appears as a sudden rise in star counts toward fainter magnitudes, so it can be found by edge detection.

3.1. Edge detection

Lee et al. (1993) located the tip by applying a Sobel filter to the binned luminosity function. With N_k the number of stars in bin k (k increasing toward fainter magnitudes), the three-point kernel $[-1, 0, +1]$ gives

$$E_k = N_{k+1} - N_{k-1}, \tag{1}$$

and the tip is placed at the strongest positive response. This kernel is equivalent, up to a factor of two, to the $[-2, 0, +2]$ form.

The result depends on the bin width and on where the bin edges fall (Makarov et al., 2006). Sakai et al. (1996) avoided binning by representing each star as a Gaussian with a width set by its photometric error, but too much smoothing can shift the measured tip, especially in noisy data (Madore et al., 2023). For our noisiest luminosity functions, we used the five-point kernel $[-2, -1, 0, +1, +2]$ (Abdollahi et al., 2026b), which spans more bins and suppresses spurious peaks.

3.2. Implementation and distance

For each galaxy, we selected stars within two half-light radii of its centre (Abdollahi, 2025, Abdollahi et al., 2026b) and within a colour window around the red giant branch (shaded band in the left panel of Figure 1). We built the i-band luminosity function with 0.05 mag bins, applied the Sobel filter, and took the

doi: https://doi.org/10.52526/25792776-26.73.2-322

strongest response as the tip, after checking the luminosity function for competing peaks. Figure 1 shows the result for And XII. Spurious detections become more likely when few RGB stars lie near the tip and photometric errors are large (Madore et al., 2023), which affects the faintest satellites in our sample. Savino et al. (2022) also found that TRGB distances to galaxies fainter than $M_V \approx -9.5$ can be biased by up to 35 per cent.

We then computed the distance modulus as

$$\mu = m_{\mathrm{TRGB}} - A_i - M_{\mathrm{TRGB}}, \tag{2}$$

where M_{TRGB} is the absolute tip magnitude in the SDSS i band, which depends only weakly on metallicity for old, metal-poor populations (Bellazzini, 2008, Lee et al., 1993). The adopted values are listed in Table 1. The foreground extinction is $A_i = 1.698\,E(B-V)$, with $E(B-V)$ from Schlegel et al. (1998) and the coefficient of Schlafly & Finkbeiner (2011) for $R_V = 3.1$. The uncertainties on μ include only the tip measurement, not the systematic uncertainties of M_{TRGB} and of the extinction correction.

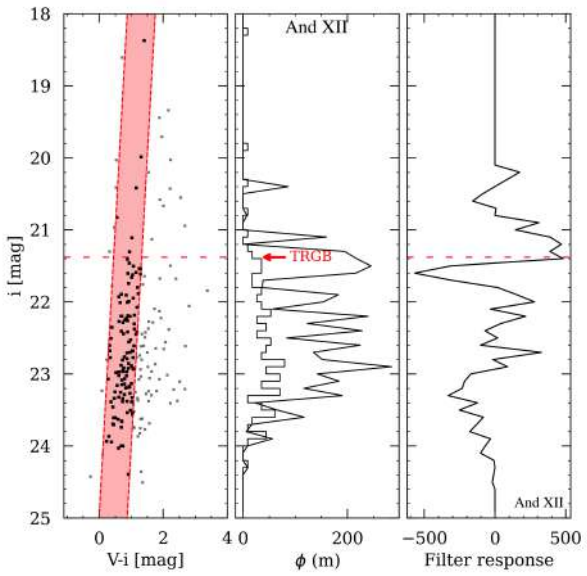

Figure 1. TRGB measurement for And XII. Left: stars within two half-light radii; the shaded band is the RGB colour window. Middle: i-band luminosity function. Right: Sobel filter response; the red line marks the TRGB.

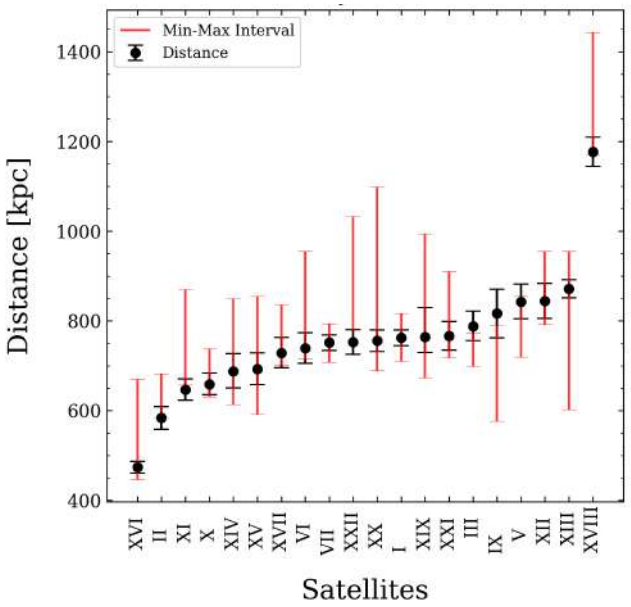

Figure 2. TRGB distances of the M31 satellites from this work (black circles) compared with the range of published values for each galaxy (red bars; values in Table 1).

4. Results

Table 1 lists the TRGB magnitudes and distances of the 17 satellites measured here, together with And I, And VII and And IX from earlier survey papers (marked with a star). The distance moduli range from 23.38 ± 0.06 mag (And XVI, 474 kpc) to 25.35 ± 0.06 mag (And XVIII, 1177 kpc), and 15 of the 20 galaxies lie between 650 and 850 kpc, around the distance of M31.

Figure 2 compares our distances with published values. For most satellites, our distance lies within the published range or agrees with at least one earlier estimate. And XVIII falls just below the range, but agrees with Conn et al. (2012) within the uncertainties. The earlier values come from several methods (TRGB, RR Lyrae, horizontal branch and CMD fitting) and telescopes, so this agreement is a useful check on our single, uniform analysis.

The closest comparison is with Conn et al. (2012), who also measured the tip in the i band. For 12 of the 18 galaxies in common, our tip is brighter by up to 0.39 mag (And XI). Six of these differences lie within 1σ and ten within 2σ; only And II (0.29 mag) and And XVI (0.22 mag) exceed 2σ. In the opposite direction, our tip for And IX is 0.59 mag fainter (1.7σ). Crowding may explain part of the offset: two red

Table 1. TRGB magnitudes and distances of the targets, compared with published values.

Galaxy	TRGB $_{this\ work}$ (mag)	$\mu_{this\ work}$ (mag) Distance (kpc)	TRGB^a (mag)	μ_{Min} (mag) Distance (kpc)	μ_{Max} (mag) Distance (kpc)	$M_{\rm TRGB}$ (mag)	A_i (mag)
And I*	21.00 ± 0.05	24.41 ± 0.05 $762.08^{+17.75}_{-17.35}$	20.98 ± 0.05	24.31 ± 0.05 [a] 727.28 ± 16.95	24.56 ± 0.09 [b] 816.58 ± 34.56	-3.50	0.090
And II	20.40 ± 0.10	23.83 ± 0.10 $584.45^{+27.54}_{-26.31}$	20.69 ± 0.05	23.83 ± 0.42 [c] 583.96 ± 54.69	24.17 ± 0.12 [b] 682.34 ± 38.77	-3.53	0.104
And III	21.14 ± 0.09	24.48 ± 0.09 $788.21^{+33.36}_{-32.00}$	20.98 ± 0.07	24.18 ± 0.11 [d] 685.44 ± 30.98	24.48 ± 0.19 [b] 787.17 ± 68.41	-3.43	0.094
And V	21.27 ± 0.10	24.63 ± 0.10 $842.46^{+39.70}_{-37.92}$	21.17 ± 0.07	24.35 ± 0.07 [a] 741.31 ± 24.29	24.66 ± 0.13 [e] 855.07 ± 52.75	-3.57	0.212
And VI	21.01 ± 0.10	24.34 ± 0.10 $738.93^{+34.83}_{-33.26}$	-	24.37 ± 0.09 [d] 748.17 ± 31.66	24.94 ± 0.09 [f] 973.99 ± 40.42	-3.44	0.107
And VII*	21.30 ± 0.05	24.38 ± 0.05 $751.62^{+17.51}_{-17.11}$	-	24.25 ± 0.25 [g] 707.95 ± 86.38	24.50 ± 0.10 [h] 794.33 ± 37.43	-3.41	0.329
And IX*	21.20 ± 0.15	24.56 ± 0.15 $816.58^{+58.40}_{-54.50}$	20.61 ± 0.31	23.89 ± 0.31 [a] 599.79 ± 92.04	24.48 ± 0.20 [i] 787.05 ± 75.93	-3.49	0.128
And X	20.77 ± 0.08	24.09 ± 0.08 $659.19^{+24.74}_{-23.84}$	20.95 ± 0.28	24.01 ± 0.07 [j] 633.87 ± 20.77	24.23 ± 0.10 [k] 701.46 ± 33.05	-3.54	0.219
And XI	20.75 ± 0.08	24.05 ± 0.08 $646.89^{+24.28}_{-23.40}$	21.14 ± 0.31	24.17 ± 0.09 [d] 682.34 ± 28.87	24.70 ± 0.20 [l] 870.96 ± 84.03	-3.44	0.136
And XII	21.38 ± 0.10	24.63 ± 0.10 $843.90^{+39.77}_{-37.99}$	21.63 ± 0.34	24.44 ± 0.12 [f] 773.76 ± 47.26	24.84 ± 0.34 [a] 928.97 ± 157.46	-3.44	0.187
And XIII	21.40 ± 0.05	24.70 ± 0.05 $871.27^{+20.29}_{-19.83}$	21.30 ± 0.07	24.40 ± 0.49 [a] 758.58 ± 192.02	24.80 ± 0.35 [m] 912.01 ± 159.51	-3.44	0.140
And XIV	20.85 ± 0.12	24.19 ± 0.12 $688.06^{+39.10}_{-37.00}$	21.18 ± 0.56	24.33 ± 0.33 [n] 734.51 ± 120.56	24.50 ± 0.56 [a] 794.33 ± 233.71	-3.44	0.101
And XV	20.84 ± 0.11	24.21 ± 0.11 $692.43^{+35.98}_{-34.20}$	21.02 ± 0.05	23.98 ± 0.26 [a] 625.17 ± 79.52	24.66 [o] 855.07	-3.45	0.079
And XVI	20.05 ± 0.06	23.38 ± 0.06 $473.79^{+13.27}_{-12.91}$	20.27 ± 0.08	23.30 ± 0.19 [a] 457.09 ± 41.80	23.72 ± 0.09 [p] 554.62 ± 23.47	-3.44	0.113
And XVII	21.00 ± 0.10	24.31 ± 0.10 $728.67^{+34.34}_{-32.80}$	21.12 ± 0.07	24.31 ± 0.11 [a] 727.78 ± 37.82	24.50 ± 0.10 [q] 794.33 ± 37.43	-3.44	0.126
And XVIII	22.09 ± 0.06	25.35 ± 0.06 $1176.74^{+32.97}_{-32.07}$	22.20 ± 0.08	25.42 ± 0.08 [a] 1213.39 ± 45.54	25.66 ± 0.13 [r] 1355.19 ± 83.61	-3.44	0.180
And XIX	21.08 ± 0.10	24.41 ± 0.10 $763.74^{+35.99}_{-34.38}$	21.24 ± 0.09	24.52 ± 0.23 [s] 801.68 ± 89.57	24.85 ± 0.13 [r] 933.25 ± 57.58	-3.44	0.105
And XX	21.05 ± 0.07	24.39 ± 0.07 $755.62^{+24.75}_{-23.97}$	21.03 ± 0.08	24.35 ± 0.16 [a] 741.31 ± 56.68	24.52 ± 0.74 [r] 801.68 ± 325.52	-3.44	0.100
And XXI	21.14 ± 0.09	24.42 ± 0.09 $766.33^{+32.43}_{-31.11}$	21.19 ± 0.07	24.40 ± 0.17 [v] 758.58 ± 61.77	24.67 ± 0.13 [t] 859.01 ± 53.00	-3.44	0.158
And XXII	21.07 ± 0.08	24.38 ± 0.08 $752.54^{+28.24}_{-27.24}$	21.11 ± 0.07	24.65 ± 0.07 [u] 853 ± 26	24.87 ± 0.09 [u] 940.12 ± 41.70	-3.44	0.133

TRGB^a is the i-band tip magnitude of Conn et al. (2012). $M_{\rm TRGB}$ is the adopted absolute tip magnitude in Eq. (2). Uncertainties on $\mu_{this\ work}$ include only the tip measurement. Literature values are from: a (Conn et al., 2012), b (Martínez-Vázquez et al., 2017) , c (Koenig et al., 1993), d (Dambis et al., 2013), e (Ferrarese et al., 2000), f (Weisz et al., 2014), g (Tikhonov & Karachentsev, 1999), h (Jacobs et al., 2009), i (Zucker et al., 2004), j (Brasseur et al., 2011), k (Zucker et al., 2007), l (Martin et al., 2006), m (Collins et al., 2010), n (Majewski et al., 2007), o (Skillman et al., 2017), p (Monelli et al., 2016), q (Irwin et al., 2008), r (McConnachie et al., 2008), s (Cusano et al., 2013), t (Martin et al., 2009), u (Chapman et al., 2013), and v (Cusano et al., 2015).

Galaxies marked with a star were previously studied by the INT group: And I (Saremi et al., 2021), And VII (Navabi et al., 2021), and And IX (Abdollahi et al., 2023). A_i was computed from $E(B-V)$ of Schlegel et al. (1998) with the coefficient of Schlafly & Finkbeiner (2011).

giants just below the tip that blend into one source look brighter than the tip and pull the edge to brighter magnitudes (Madore et al., 2023). Our INT images (0.33 arcsec pixels) can be more affected by blending in the galaxy centres than the PAndAS CFHT/MegaCam data used by Conn et al. (2012), which have finer pixels and cover each galaxy fully. The different methods, a Bayesian fit in Conn et al. (2012) and a Sobel filter here, may also play a role.

5. Discussion and conclusions

We have presented TRGB distances to 17 satellites of M31 from the i-band photometry of the INT monitoring survey, and combined them with earlier survey distances for three more. Most are consistent with at least one published estimate, and the common data set and analysis give a homogeneous basis for comparing these galaxies. Our tips tend to be brighter than those of Conn et al. (2012); crowding and the different methods may contribute, but the comparison alone does not establish the cause.

The revised distances have particular implications for three systems. And XII lies about 60 kpc behind M31 (for an M31 distance of ~ 780 kpc), which is only about 1.5σ given our uncertainty; the earlier value of Conn et al. (2012) placed it farther behind. Our result is therefore consistent with the first-infall interpretation discussed by Chapman et al. (2007), but does not add strong new support to it.

And XXII is closer than all previous estimates. Its projected separation from M33 is 42 kpc (Martin et al., 2009). Adopting the M33 distance of 794 ± 23 kpc used in recent M31–M33 orbit models (as summarised by Savino et al., 2022), our distance gives a three-dimensional separation of about 59 kpc, compared with about 72 kpc for the distance of 853 kpc from Chapman et al. (2013). Our result therefore keeps And XXII close to M33. However, Savino et al. (2022) found that the M33 distance differs significantly from this value, so this separation depends on the adopted M33 distance, and the association cannot be established from distance alone (Chapman et al., 2013).

And XVIII is closer than all previous estimates, but it still lies about 400 kpc behind M31. Its membership in the M31 system therefore remains uncertain. Its distance at discovery was even larger (McConnachie et al., 2008).

Together with the census of approximately 2800 LPV candidates across 17 M31 satellites, these distances contribute to a homogeneous characterization of the stellar populations in the Andromeda satellite system. Further constraints on membership will require the distances to be combined with kinematics and three-dimensional positions.

References

Abdollahi H., 2025, Communications of the Byurakan Astrophysical Observatory, 72, 416

Abdollahi H., Javadi A., Mirtorabi M. T., et al., 2023, Astrophys. J. , 948, 63

Abdollahi H., Javadi A., van Loon J. T., McDonald I., Abdollahi M., Saremi E., Khosroshahi H. G., Mahani H., 2024, Communications of the Byurakan Astrophysical Observatory, 71, 383

Abdollahi H., et al., 2026a, VizieR Online Data Catalog: INT survey of local dwarf gal. VIII. LPV stars (Abdollahi+, 2026), VizieR On-line Data Catalog: J/ApJ/1000/69. Originally published in: 2026ApJ..1000...69A

Abdollahi H., Javadi A., van Loon J. T., et al., 2026b, Astrophys. J. , 1000, 69

Bellazzini M., 2008, Mem. Soc. Astron. Italiana, 79, 440

Brasseur C. M., Martin N. F., Rix H.-W., Irwin M., Ferguson A. M. N., McConnachie A. W., de Jong J., 2011, Astrophys. J. , 729, 23

Chapman S. C., et al., 2007, Astrophys. J. Lett. , 662, L79

Chapman S. C., et al., 2013, Mon. Not. R. Astron. Soc. , 430, 37

Collins M. L. M., et al., 2010, Mon. Not. R. Astron. Soc. , 407, 2411

Conn A. R., et al., 2012, Astrophys. J. , 758, 11

Cusano F., et al., 2013, Astrophys. J. , 779, 7

Cusano F., Garofalo A., Clementini G., Cignoni M., et al., 2015, Astrophys. J. , 806, 200

Dambis A. K., Berdnikov L. N., Kniazev A. Y., Kravtsov V. V., Rastorguev A. S., Sefako R., Vozyakova O. V., 2013, Mon. Not. R. Astron. Soc. , 435, 3206

Erben T., et al., 2005, Astronomische Nachrichten, 326, 432

Ferrarese L., et al., 2000, Astrophys. J. , 529, 745

Irwin M. J., Ferguson A. M. N., Huxor A. P., Tanvir N. R., Ibata R. A., Lewis G. F., 2008, Astrophys. J. Lett. , 676, L17

Jacobs B. A., Rizzi L., Tully R. B., Shaya E. J., Makarov D. I., Makarova L., 2009, Astron. J. , 138, 332

Javadi A., van Loon J. T., Mirtorabi M. T., 2011a, Mon. Not. R. Astron. Soc. , 411, 263

Javadi A., van Loon J. T., Mirtorabi M. T., 2011b, Mon. Not. R. Astron. Soc. , 414, 3394

Javadi A., van Loon J. T., Khosroshahi H., Mirtorabi M. T., 2013, Mon. Not. R. Astron. Soc. , 432, 2824

Javadi A., van Loon J. T., Khosroshahi H. G., Tabatabaei F., Hamedani Golshan R., Rashidi M., 2017, Mon. Not. R. Astron. Soc. , 464, 2103

Koenig C. H. B., Nemec J. M., Mould J. R., Fahlman G. G., 1993, Astron. J. , 106, 1819

Landolt A. U., 1992, Astron. J. , 104, 340

Lee M. G., Freedman W. L., Madore B. F., 1993, Astrophys. J. , 417, 553

Madore B. F., Freedman W. L., Owens K. A., Jang I. S., 2023, Astron. J. , 166, 2

Mahani H., Javadi A., 2026, SEDust: SED fitting of AGB stars with DUSTY, Astrophysics Source Code Library, record ascl:2605.024 (ascl:2605.024)

Mahani H., et al., 2023, IAU, 373, 264

Mahani H., et al., 2025, Astrophys. J. , 992, 94

Mahani H., Javadi A., Abdollahi H., Khatamsaz F., 2026, Iranian Journal of Physics Research, 26, 237

Majewski S. R., et al., 2007, Astrophys. J. Lett. , 670, L9

Makarov D., Makarova L., Rizzi L., Tully R. B., Dolphin A. E., Sakai S., Shaya E. J., 2006, Astron. J. , 132, 2729

Martin N. F., Ibata R. A., Irwin M. J., Chapman S., Lewis G. F., Ferguson A. M. N., Tanvir N., McConnachie A. W., 2006, Mon. Not. R. Astron. Soc. , 371, 1983

Martin N. F., et al., 2009, Astrophys. J. , 705, 758

Martínez-Vázquez C. E., et al., 2017, Astrophys. J. , 850, 137

McConnachie A. W., 2012, Astron. J. , 144, 4

McConnachie A. W., et al., 2008, Astrophys. J. , 688, 1009

Monelli M., et al., 2016, Astrophys. J. , 819, 147

Navabi M., et al., 2021, Astrophys. J. , 910, 127

Rostami N., Mahani H., 2025, Communications of the Byurakan Astrophysical Observatory, 72, 381

Sakai S., Madore B. F., Freedman W. L., 1996, Astrophys. J. , 461, 713

Saremi E., et al., 2020, Astrophys. J. , 894, 135

Saremi E., Javadi A., Navabi M., van Loon J. T., Khosroshahi H. G., Bojnordi Arbab B., McDonald I., 2021, Astrophys. J. , 923, 164

Savino A., Weisz D. R., Skillman E. D., et al., 2022, Astrophys. J. , 938, 101

Schlafly E. F., Finkbeiner D. P., 2011, Astrophys. J. , 737, 103

Schlegel D. J., Finkbeiner D. P., Davis M., 1998, Astrophys. J. , 500, 525

Skillman E. D., et al., 2017, Astrophys. J. , 837, 102

Stetson P. B., 1987, Publ. Astron. Soc. Pac. , 99, 191

Stetson P. B., 1994, Publ. Astron. Soc. Pac. , 106, 250

Tikhonov N. A., Karachentsev I. D., 1999, Astronomy Letters, 25, 332

Weisz D. R., Dolphin A. E., Skillman E. D., Holtzman J., Gilbert K. M., Dalcanton J. J., Williams B. F., 2014, Astrophys. J. , 789, 147

Zucker D. B., et al., 2004, Astrophys. J. Lett. , 612, L121

Zucker D. B., et al., 2007, Astrophys. J. Lett. , 659, L21